Dynamic and static light scattering analysis of DNA ejection from the phage λ

David Löf,[1] Karin Schillén,[1,*] Bengt Jönsson,[2] and Alex Evilevitch[3,*]
[1]*Division of Physical Chemistry 1, Center for Chemistry and Chemical Engineering, Lund University, P.O. Box 124, SE-221 00 Lund, Sweden*
[2]*Division of Biophysical Chemistry, Center for Chemistry and Chemical Engineering, Lund University, P.O. Box 124, SE-221 00 Lund, Sweden*
[3]*Division of Biochemistry, Center for Chemistry and Chemical Engineering, Lund University, P.O. Box 124, SE-221 00 Lund, Sweden*
(Received 13 January 2007; revised manuscript received 27 April 2007; published 20 July 2007)

With the aid of time-resolved dynamic light scattering (DLS) and static light scattering (SLS), we have analyzed the ejection kinetics from the bacterial virus bacteriophage (or phage) λ, triggered *in vitro* by its receptor. We have used DLS to investigate the kinetics in such a system. Furthermore, we have shown that both SLS and DLS can be interchangeably used to study the process of phage DNA release. DLS is superior to SLS in that it also allows the change in the light scattering arising from each of the components in the system to be monitored under conditions such that the relaxation times are separable. With help of these two methods we present a model explaining the reason for the observed decrease in the scattering intensity accompanying DNA ejection from phage. We emphasize that ejection from phage capsid occurs through a very long tail (which is nearly three times longer than the capsid diameter), which significantly separates ejected DNA from the scattering volume of the capsid. The scattering intensity recorded during the DNA ejection process is the result of a change in the form factor of the phage particle, i.e., the change in the interference effects between the phage capsid and the DNA confined in the phage particle. When the DNA molecule is completely ejected it remains in the proximity of the phage for some time, thus contributing to the scattering signal as it diffuses away from the phage capsid, into the scattering volume and returns to its unperturbed chain conformation in bulk solution. The free DNA chain does not contribute to the scattered intensity, when measured at a large angle, due to the DNA form factor and the low concentration. Although the final diffusion-controlled step can lead to overestimation of the real ejection time, we can still use both scattering methods to estimate the initial DNA ejection rates, which are mainly dependent on the pressure-driven DNA ejection from the phage, allowing studies of the effects of various parameters affecting the ejection.

DOI: 10.1103/PhysRevE.76.011914 PACS number(s): 82.39.Pj, 87.64.Cc

I. INTRODUCTION

Light scattering techniques have proved to be important and extremely powerful tools in characterizing and exploring the microdomains and macrodomains of biology for several decades [1–5]. Particularly dynamic light scattering (DLS) has proven to be a useful method of investigating the solution dynamics of DNA (deoxyribonucleic acid), where both translational and internal dynamics (rotational motion and intramolecular relaxation) of short DNA fragments have been studied [6–10]. Highly negatively charged DNA (one charge per 0.17 nm) is a linear polyelectrolyte of great importance since it is the carrier of genetic information. There is, therefore, a considerable interest in investigating DNA condensation using different materials with the purpose of replacing viral vectors as gene carriers for *in vivo* gene transfer (see, for example, Refs. [11–13], and the references therein). We have also employed DLS in various physicochemical studies involving DNA and its interactions with other substances that change the conformation of DNA. It was, for example, used to investigate the cationic surfactant-induced compaction of salmon sperm DNA [2000 base pairs (BP)], both in bulk solution as well as on different polystyrene particle surfaces [14,15]. Surfactant-induced compaction studies of DNA with longer chain lengths has also been performed by others using DLS [16]. The advantage of DLS is that the diffusion by scattering objects of different sizes can be detected simultaneously, a fact that was used in our investigation of the thiol-specific and nonspecific interactions between DNA and gold nanoparticles [17], and recently also in a DLS and fluorescence spectroscopic study of DNA compaction through the complex formation between 2 kbp DNA and poly(amidoamine) dendrimers [18]. In this study, we have analyzed the kinetics of DNA ejection from the λ bacterial virus (or phage) using time-resolved DLS and compared the results to data obtained with time-resolved static light scattering (SLS).

All viruses consist of a viral genome contained in a protein shell, or capsid. Almost all plant and animal viruses infect cell by the whole viral particle entering the cell, where the viral genome is released from the capsid. Bacteriophages, on the other hand, remain outside the cell and infect it by injecting their genome into the cell [19]. Although phages have played a major role in the development of microbiology and molecular biology, it is still not fully understood how the phage genome finds its way into the cell.

In most cases, DNA is highly compacted inside the phage capsid. The conformation and state of stress of the packed viral DNA has been investigated theoretically [20–29]. We

*Corresponding authors: Karin.Schillen@fkem1.lu.se and Alex.Evilevitch@biochemistry.lu.se

have recently shown experimentally that DNA ejection from the phage λ *in vitro* is driven mainly by a mechanical force arising from bending and electrostatic DNA-DNA repulsion forces acting on the DNA, which is packed to almost crystalline densities inside the capsid [30,31]. We have also measured this internal DNA pressure and found it to be on the order of tens of atmospheres [30]. In parallel, in another *in vitro* experiment, it was shown that forces of the same magnitude were required to package DNA into the phage $\phi 29$ [32]. Based on these empirical observations, one could conclude that infection by phages is achieved by the internal ejection force of the confined phage DNA.

However, recent experimental [33] and theoretical [34] studies suggest that despite high internal DNA pressure in phages, the ejection of viral DNA into bacterial cytoplasm could not be completely achieved due to the counterbalancing osmotic pressure of at least 2 atm in the cell [35]. This osmotic pressure would be sufficient to prevent almost 50% of λ-DNA from being injected [34,36]. In order to better understand the mechanism of DNA ejection *in vivo*, it would be fruitful to systematically investigate the effects of various internal and external factors affecting the DNA ejection process. Such an analysis can be performed by studying the kinetics of DNA ejection from phages under different conditions.

Time-resolved static light scattering has previously been successfully employed to investigate DNA ejection from the bacteriophage T5 [37,38]. With SLS, the time-averaged intensity of the scattered light arising from the sum of all components present in the scattering volume is measured. In DLS, based on the photon correlation spectroscopy technique, a time correlation function of the scattering intensity is constructed, which contains scattering information on each component (their relative contributions to the total scattering intensity), as well as the separate translational diffusion coefficients. Therefore, DLS has an advantage, in that it provides a direct indication of the change in scattering of each component during the kinetic process of ejection. At present, however, neither the DLS nor the SLS measurements performed in this work permit us to relate the fraction of DNA remaining in the capsid to the measured scattering intensity signal (as in fluorescence studies [39]), due to the contributions to the signal from DNA both inside and outside the phage (since we also observe slower DNA diffusion away from the phage after ejection, see discussion below). However, with help of our data we present here a model showing that during the initial stage of the ejection process, the change in the scattering intensity will be mainly attributed to the ejection of DNA from the phage, during which the form factor of the phage particle will change. This will thus allow the evaluation of the kinetics of ejection by analyzing the initial ejection rates derived from the slopes of the changing scattering signal obtained from both SLS and DLS. In this paper we focus especially on the DLS results. We are currently working on a theoretical model that will allow us to directly relate the scattering intensity to the amount of DNA remaining in the capsid. From this model, we will learn to what extent the DLS and SLS data presented here can be used to precisely describe the rate of DNA ejection from a phage through out the entire ejection process.

The goal of this study was not to determine the absolute duration of the ejection process but to show that both static and dynamic light scattering techniques offer new means of studying the kinetics of viral ejection and with their help find coupling between the observed scattering data and the ejection process. These methods allow us to make qualitative comparisons of the initial ejection rates under different physical conditions, without the need to use DNA intercalating or groove-binding dyes as required in fluorescence spectroscopy. Moreover, it has recently been shown that fluorescent dyes can further complicate the interpretation of ejection data by rupturing the phage particles and introducing additional kinetic effects due to competition with DNA counterions and DNA-binding proteins [40].

II. EXPERIMENT

A. Bacteriophage strain and preparation of phage stock

Wild type (wt) λ cI857 bacteriophages, with a genome length of 48.5 kbp and its shorter genome mutant with 45.7 kbp (corresponding to 94% of the wt DNA), were produced by thermal induction of the lysogenic *Escherichia coli* strains AE1 and AE2 [33]. Both strains were modified to grow without LamB protein expressed on their surface in order to increase the yield of phage induced in the cell. The culture was then lysed by temperature induction. Phage λ with 37.7 kbp DNA (corresponding to 78% of the wt DNA) (denoted λb221) was extracted from single plaques. The phage purification details are described elsewhere [30]. The phage samples were purified by CsCl equilibrium centrifugation and thereafter dialyzed from CsCl against TM (tris-magnesium) buffer (10 mM $MgSO_4$ and 50 mM tris-HCl/pH7.4). The final titer was 10^{12} virions/mL, as determined by plaque assay [41].

B. Preparation of phage λ receptor (LamB)

The receptor was the LamB protein purified from pop 154, a strain of *E. coli* K12 in which the *lamB* gene has been transduced from *Shigella sonnei* 3070 [42,43]. This protein occurs as a trimer with a total molecular weight of 141 kDa (47 kDa per monomer) [44]. It has been shown to cause complete *in vitro* ejection of DNA from the phage λ in the absence of the solvents required with the wild-type *E. coli* receptor [44,45]. Purified LamB was solubilized from the outer membrane with a 1% solution (by volume) of the nonionic surfactant, n-octylpolyoxyethylene (oPOE) $[CH_3(CH_2)_7(OCH_2CH_2)_nOH$ $(n=2-9)]$ [46].

C. Sample preparation

The bacteriophage λ was solubilized in TM buffer to a final concentration of $\approx 10^{10}$ virions/mL. In order to maintain the same oPOE micellar concentration in the final phage-receptor solution in the ejection experiments (where the micellized receptor solution is added to the phage solution), the oPOE surfactant was added to the phage solution to a concentration of 1%, by volume (as with the receptor solution). Prior to the light scattering measurements, the phage-

oPOE solution was filtered directly into the cylindrical light-scattering quartz cell through a sterile, hydrophilic Minisart filter with a 0.2 μm pore diameter (Sartorius, Germany). The ejection of DNA from the phage was triggered by adding 60 μL of 20 μg/mL LamB receptor solubilized in oPOE micelles (at a ratio corresponding to 1 phage: 100 LamB trimers) to 1 mL of phage solution directly to the light-scattering cell. The sample was mixed by gently tapping the cell. The DLS and SLS measurements were started 30 s after the receptor had been added and mixed with the phage-oPOE solution. In order to check that the receptor was in excess and that the phage-receptor binding is not rate-limiting [39], the ejection kinetics was measured with 20 μL of LamB instead of 60 μL and it was found that the rates of ejection were identical in both cases.

D. Dynamic and static light scattering

The setup used for the DLS and SLS measurements employed an ALV/DLS/SLS-5000F, CGF-8F-based compact goniometer system from ALV-GmbH, Langen, Germany with vertical-vertical polarization geometry. The light source was a diode-pumped Nd:YAG solid-state Compass-DPSS laser (Coherent Inc., Santa Clara, California), which operates at 532 nm with a fixed output power of 400 mW that can be varied using an attenuator from Newport Inc. The cylindrical quartz cell is immersed in a refractive-index-matching liquid (cis-decahydronaphthalene or decaline) contained in a cylindrical quartz container (VAT). The detection system includes a near-monomodal optical fiber and two matched photomultipliers in a pseudo-cross geometry. The temperature was 25 °C, which was controlled to within ±0.01 °C. A detailed description of the DLS/SLS equipment can be found in Ref. [47].

In a DLS measurement, the time correlation function (TCF) of the intensity of the scattered light is measured. The model used in the fitting procedure is, however, expressed with respect to the normalized TCF of the electric field $g^{(1)}(t)$, which is related to the normalized intensity TCF $g^{(2)}(t)$ by Siegert's relation [48]:

$$g^{(2)}(t) - 1 = \beta |g^{(1)}(t)|^2, \tag{1}$$

where t is the lag time and β is the coherence factor ($\leqslant 1$) that takes into account deviations from the ideal correlation and the experimental geometry.

$g^{(1)}(t)$ can either be a single exponential function, with one corresponding relaxation time τ or a multiexponential decay depending on the system investigated. For a system that exhibits a distribution of relaxation times, $g^{(1)}(t)$ may be described by a Laplace transform [49]

$$g^{(1)}(t) = \int_0^\infty A(\tau)\exp(-t/\tau)d\tau = \int_{-\infty}^\infty \tau A(\tau)\exp(-t/\tau)d\ln\tau, \tag{2}$$

where $\tau = \Gamma^{-1}$, and Γ is the relaxation rate or frequency.

The relaxation time distribution $A(\tau)$ can be obtained by performing an inverse Laplace transformation of the measured intensity correlation function $g^{(2)}(t)$ using the nonlinear constrained regularization method REPES, in which the sum of the differences between the experimental and calculated $g^{(2)}(t)$ functions is minimized [49–51]. REPES is incorporated into the GENDIST analysis package [52], but an upgraded version of REPES, which was a kind gift from P. Štěpánek, was also used in this study [53]. REPES iterates a penalizing parameter to the probability of rejecting the penalized solution selected by the user. In this study, we varied the "probability-to-reject" term from low values ($\sim 10^{-8}$) up to 0.5. The relaxation time distributions presented are expressed in equal area representation as $\tau A(\tau)$ vs $\log_{10}[\tau(\text{ms})]$ [49].

When the distribution contains several relaxation modes (translational diffusion or other modes), the relative area of each mode, which corresponds to the pre-exponential amplitude A_n (where $n=1-\infty$) of a multiexponential intensity correlation function, is given by the analysis, see Eq. (2). Each relaxation process thus has an amplitude associated with it, and therefore also a relative scattered intensity, expressed as the amplitude multiplied by the time-averaged total scattering intensity I ($I_n = A_n I$). We have monitored the change in the relative amplitudes during the DLS measurements as a function of time in order to calculate the individual scattering intensity of the phage particles and the receptors (solubilized in oPOE surfactants) in order to study the kinetics of the ejection of DNA from the phage λ.

From the relaxation rate, Γ, obtained from the REPES analysis, the apparent translational diffusion coefficient D can be calculated:

$$D = \lim_{q\to 0}\left(\frac{\Gamma}{q^2}\right), \tag{3}$$

where q is the absolute value of the scattering vector [$q = 4\pi n_0 \sin(\theta/2)/\lambda$, where n_0 is the refractive index of the solvent (here water), λ is the incident wavelength and θ is the scattering angle].

Γ is measured at different values of q (i.e., different angles) and D is evaluated from the slope of $\Gamma = f(q^2)$. The apparent hydrodynamic radius $R_{H,\text{app}}$ at a finite concentration can be estimated from D using the Stokes-Einstein relation

$$R_{H,\text{app}} = \frac{kT}{6\pi\eta_0 D}, \tag{4}$$

where k denotes Boltzmann's constant, T is the absolute temperature, and η_0 is the viscosity of water. When measurements are performed under highly diluted conditions, as in this case, intraparticle interactions can be neglected, and D is close to that at infinite dilution, and Eq. (4) gives R_H directly.

III. RESULTS AND DISCUSSION

As a starting point, we first characterize the static and hydrodynamic properties of three λ phages containing DNA of various lengths (78, 94, and 100% of the wt DNA length, 48.5 kbp) in solution at equilibrium without the receptor present using SLS and DLS. The purpose of the SLS measurements was to determine the radius of gyration of the different phages, i.e., to compare their form factors, which reflects how the DNA content inside the phage affects the

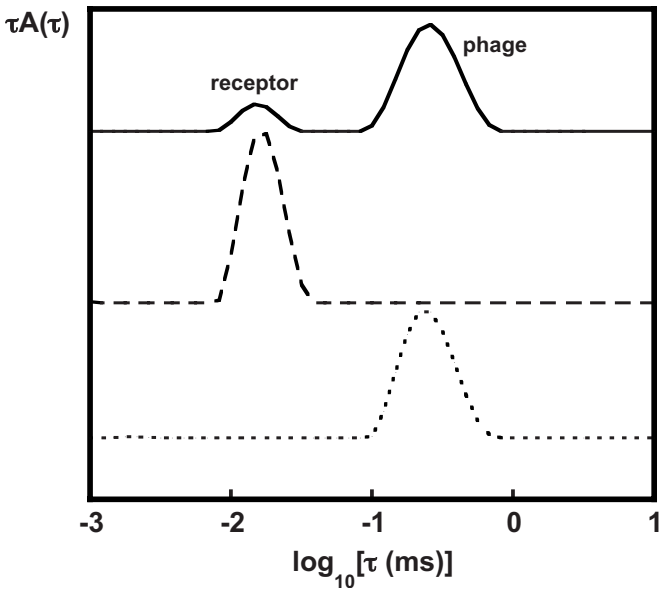

FIG. 1. Relaxation time distributions obtained from inverse Laplace transformation of intensity correlation functions from DLS for the phage λ with 48.5 kbp DNA in an aqueous solution containing $\sim 10^{10}$ virions/mL phage (dotted line), micellized LamB receptor in aqueous solution containing 1.2 μg/mL LamB and 1% (v/v) oPOE surfactant (dashed line) and $\sim 10^{10}$ virions/mL phage aqueous solution with 1% (v/v) oPOE (solid line). (Measurements at 25 °C and at θ=90°. The "probability-to-reject" term=0.5.)

scattering intensity. The purpose of the DLS measurements on the equilibrium system (phage and oPOE micelles) was to determine the hydrodynamic size of each component. Furthermore, information is obtained on the relative scattering contributions before the receptor is added from the relaxation time distributions.

A. Sample characterization

Dynamic light scattering. The DLS technique was used to characterize the hydrodynamic size of the bacteriophage λ both in pure aqueous solution and in the mixed solution containing the oPOE surfactant micelles. The size of the oPOE micelles containing the receptor LamB was also investigated. In Fig. 1, the relaxation time distributions obtained from the inverse Laplace transformation of the intensity correlation functions are shown for the mixed solution of phage and pure oPOE micelles (top), the oPOE micellar solution with the receptor (middle) and the pure phage λ solution (bottom). The distributions of the phage and receptor-oPOE micellar solution are monomodal, whereas a bimodal distribution is seen for the mixture. The faster mode at short times is attributed to the translational diffusion of the micelles and the slower mode at longer times to the diffusion of the phages. In the receptor-oPOE micellar solution (denoted the "micellized receptor" solution, for simplicity), both pure oPOE micelles and receptor-oPOE complexes are present. The contribution of the receptor-oPOE complexes to the scattering intensity of the mixed solution is considered to be negligible as the number of receptors used is far below the number of oPOE micelles (approximately 10 000 times lower, obtained by simple geometrical calculations either using the micellar radius obtained from DLS or the estimated headgroup area). Only a minor, and hence negligible, increase in the total intensity was observed as a result of the increasing number of scattering particles. Thus, no effect was found on the measured hydrodynamic radius of the micelles when a portion of the receptor-oPOE micellar solution was added to a solution of pure oPOE micelles.

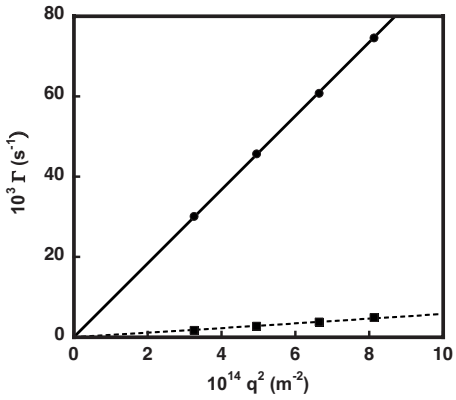

FIG. 2. The relaxation rates (Γ) for the oPOE micellar mode (●) and the phage mode (■) as a function of the square of the magnitude of the scattering vector (q^2) for a $\sim 10^{10}$ virions/mL phage solution with 1% (v/v) oPOE at 25 °C.

The hydrodynamic radii of the phage and the oPOE micelles (without LamB), in the mixed phage-oPOE solution were estimated from DLS measurements performed at different angles. The relaxation rates of the two modes are shown in Fig. 2 as a function of q^2. Both functions pass through the origin and show perfectly linear behavior, which indicates that the modes are due to translational diffusion processes. The diffusion coefficients are given by the slopes [Eq. (3)] and the apparent hydrodynamic radii are calculated using Eq. (4). $R_{H,\mathrm{app}}$ of the phage λ was estimated to be 42 nm and for the oPOE micelle 2.7 nm. Since the concentration is low, these values are considered to be close to the true R_H values. Cryogenic transmission electron microscopy (cryo EM) studies have indicated that the phage λ has an outer radius of 31.5 nm [54]. This technique gives a geometrical radius. The hydrodynamic radius obtained from DLS is the equivalent radius of a hard sphere with a solvent layer, and is defined by hydrodynamic interactions. Due to the solvating layer thickness and the fact that the value of $R_{H,\mathrm{app}}$ obtained with DLS is averaged (or intensity z-averaged), it is larger than the value obtained from cryo EM. With this in mind, we may note that the tail of the virus capsid does not seem to hinder the translational diffusion of the phage, which would give a larger value of $R_{H,\mathrm{app}}$.

Static light scattering of pure bacteriophage λ. The time-averaged static light scattering intensity $I(q)$ of a dilute solution of identical scattering particles of molar mass M is proportional to the number density, the static structure factor $S(q)$, which describes the spatial interparticle correlations and accounts for the intermolecular interactions, and the form factor $P(q)$ that describes the interference effects within the scatterers and contains information about their size and

shape: $I(q) \propto NP(q)S(q)$, where N is the number of particles in the scattering volume (q is, as before, the magnitude of the scattering vector).

In an SLS experiment the measured intensity is often expressed in terms of the Rayleigh ratio R_θ, defined as [55,56]

$$R_\theta = \frac{I(q)}{I_{\text{tol}}(q)} R_{\text{tol}} \left(\frac{n_0}{n_{\text{tol}}} \right)^2, \tag{5}$$

where $I_{\text{tol}}(q)$ is the average scattering intensity of the reference (toluene) measured at q, R_{tol} is the Rayleigh ratio of toluene, and n_0 and n_{tol} are the refractive indices of the solvent and toluene, respectively.

The Rayleigh ratio of the solution can also be expressed as $R_\theta = KcMP(q)S(q)$, where c is the solute concentration and K is an optical constant ($K = 4\pi^2 n_0^2 (dn/dc)^2 / (\lambda^4 N_A)$, where dn/dc is the refractive index increment and N_A is Avogadro's constant). This equation is often used with the virial expansions of $P(q)$ [$P(q) = (1 - q^2 R_g^2/3 + \cdots)$] and $S(q)$ which give the angular and concentration dependence of the scattered intensity [57]. The radius of gyration (R_g) of the particle can be obtained from the angular dependence.

In order to characterize the pure bacteriophages at equilibrium conditions and to determine how the amount of DNA inside the phage affects the scattering from phage particles, SLS measurements were performed on three bacteriophages λ (without the micellized receptor) containing three different lengths of DNA: 37.7, 45.7, and 48.5 kbp. The measurements were carried out in dilute TM buffer solutions with the purpose of comparing the form factor (or rather R_g) of the different phages. The angular ($\theta = 40-145°$, every 5°) and concentration dependence (2–3 concentrations) of the scattering intensity was measured. In this study, the refractive index increment, dn/dc, of each phage was not determined and as a result the molar mass of the phages could not be directly evaluated. Instead, the reduced scattering intensity c/R_θ (expressed without the optical constant K) was analyzed. The apparent radius of gyration was calculated from the angular dependence of c/R_θ at each phage concentration. The value of R_g varied very little between the different concentrations, which shows that the structure factor $S(q)$ is close to one (dilute regime, no intermolecular interactions). We obtained for the three phages the following values: $R_g = 38-40$ nm (37.7 kbp), $R_g = 38-40$ nm (45.7 kbp), and $R_g = 36-40$ nm (48.5 kbp). The lack of variation in the values indicates that R_g is mostly determined by the geometry of the capsid, which is the same for all three phages, and not the DNA content.

By combining the two light-scattering radii obtained from DLS and SLS as described above, together with the well-known relation $\rho = R_g/R_H$, information about the structure of the scattering particle can be obtained [58,59]. The value of ρ is 0.778 for a homogeneous sphere, for a monodisperse random coil in theta solvent ρ is 1.73 and in a good solvent 1.78. The value of ρ for a monodisperse rigid rod is >2.0. For phage λ with 48.5 kbp DNA we obtain $\rho = 37.8/42 = 0.9$. This indicates a rather compact particle, perhaps with some flexibility originating from the tail. It was also observed in the DLS measurements that the tail does not contribute significantly to the collective translational diffusion.

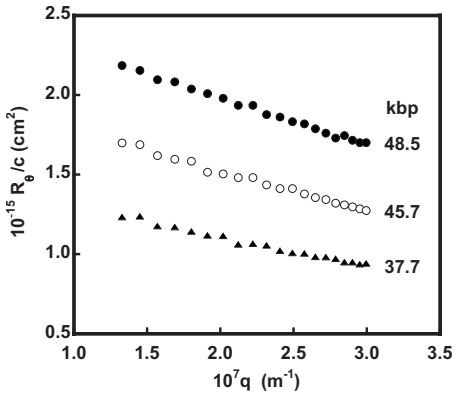

FIG. 3. Scattering data from SLS presented as the Rayleigh ratio normalized to the phage concentration (R_θ/c) as a function of the magnitude of the scattering vector (q) for three different phage λ particles in aqueous solution at 25 °C: 48.5 kbp DNA (●), 45.7 kbp DNA (○), and 37.7 kbp DNA (▲). The concentrations (expressed as $N_{\text{phage}}/\text{g}$) were 4.33×10^{10} (48.5 kbp), 4.28×10^{10} (45.7 kbp), and 3.04×10^{10} (37.7 kbp).

The SLS data can also be presented as scattering curves such as those shown in Fig. 3, where the normalized scattered intensity (Rayleigh ratio divided by the highest phage concentration expressed as the number of phage per gram $N_{\text{phage}}/\text{g}, c/R_\theta$) obtained for the three phages are given as a function of q. In this figure, a minor difference can be noted between the three phages. This means that the form factor $P(q)$ is slightly different. However, this difference is almost negligible, especially at larger angles. We will now compare the scattering intensity of each phage at the fixed scattering angle 120° (which was used in the ejection studies presented below and in Ref. [60]). With an almost constant contribution of $P(q)$ (Fig. 3), $S(q) \approx 1$ and assuming a constant value of dn/dc for the three phages, the scattering intensity at 120° is proportional to an *apparent* molecular weight of the phage M(phage). The almost linear difference in scattering intensity observed between these samples when plotted vs encapsidated DNA length may thus be mostly ascribed to the difference in molecular weight of the DNA contained in the phage capsids since the molecular weight of the empty capsid is the same in all three cases: M(phage) = M(encapsidated DNA) + M(empty capsid). This confirms that the dominant factor governing the difference in scattering intensity is the molecular weight of the confined DNA. However, since $P(q)$ may not be exactly the same for the three phages this conclusion should be treated with caution until future studies can be performed, where the low-q regime will be investigated in more detail, as well as the time-resolved angular dependence of the form factor during the ejection process (see below).

B. DNA ejection from bacteriophage λ

The ejection of the genome through the tail of the phage λ capsid was studied by performing simultaneous SLS and DLS measurements as a function of time. The measurements started 30 s after adding the LamB receptor, solubilized in

oPOE surfactant, to the phage λ solution (as described above). The receptor-mediated triggering of DNA ejection from the phage, through receptor-tail binding, followed by the conformational change of the tail proteins, is considered to be instantaneous [39].

Ejection studied with SLS. After the mixed phage-oPOE solution had been characterized, time-dependent SLS measurements were performed to investigate the kinetics of DNA ejection from phage λ. These measurements were carried out by consecutive DLS measurements with a duration of 30 s, where a recording of the total time-averaged static light scattering intensity was included, on solutions containing a mixture of scattering particles (bacteriophages, ejected DNA, and oPOE surfactant micelles with and without incorporated LamB). During 30 s, the change in the average scattering intensity is considered to be negligible. When performing these experiments under dilute conditions, the intermolecular interactions between the different scattering particles can be neglected and the total scattering intensity depends only on the average molar mass of all scattering particles, the total concentration and on the sum of the form factors of the scatterers that exhibit intraparticle interference (in this case the filled, partially filled, and empty phages and the ejected DNA). The LamB receptors (solubilized in oPOE micelles) are regarded as point scatterers. Based on the SLS results presented above, the form factor of the phage, $P(q)$ (with DNA confined) is constant only prior to ejection. Once ejection has been triggered by the receptor, the form factor of the phage will change in time as DNA is ejected. The scattering will depend on the interference between the DNA inside and outside the phage particle (the contribution to the scattering from the micellized receptor is constant, as shown in the DLS results, below).

Finally, it should be pointed out that once the ejected DNA coils have diffused away from the capsids into the bulk solution, they do not contribute to the total scattering intensity due to their low number density. In addition, all measurements were performed at $\theta=120°$, where the scattering is further reduced because of the strong angular dependence of the form factor of the large extended and unperturbed DNA coil (high destructive interference), and which leads to $qR_g \gg 1$ [61,62].

The total light scattering intensity relative to the incident laser intensity, normalized to the initial value at $t=0$ (I/I_0) as a function of time, is shown in Fig. 4 for ejection from the wt phage λ (with 48.5 kbp long DNA) at 25 °C (see the filled circles data points). It can be clearly observed that the intensity decreases as the ejection process proceeds. As will be shown below, the DLS measurements give even better insight into the ejection kinetics, since the change in the light scattering arising from each of the individual components in the system can be monitored.

Ejection studied with DLS. The DLS measurements with a duration of 30 s (including a simultaneous recording of the time-averaged light scattering intensity) were carried out at intervals of 34 s (30 s plus 4 s of autoscaling). During 30 s, the change in the relative amplitudes of each of the components obtained from the relaxation time distributions from DLS is considered to be negligible. The mean position (i.e. the relaxation time, τ) of the modes in the distribution may

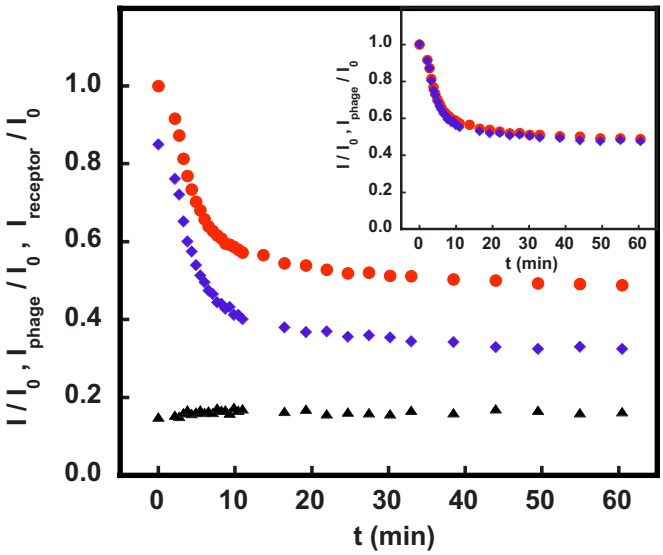

FIG. 4. (Color online) The total light scattering intensity from SLS relative to the incident laser intensity (I) normalized to the initial value at $t=0$ (I_0), I/I_0 (●), as a function of time. The normalized light scattering intensity from DLS of the phage I_{phage}/I_0 (◆) and the micellized LamB receptor $I_{receptor}/I_0$ (▲) as a function of time during the ejection of 48.5 kbp DNA. (Measurements on a $\sim 10^{10}$ virions/mL phage solution with 1% (v/v) oPOE at 25 °C and at $\theta=120°$.)

have greater uncertainty but these values are not of interest when studying the ejection process.

In Fig. 5(a), we present the relaxation time distributions obtained from the REPES analysis of the measured intensity correlation functions of the phage λ (with 48.5 kbp DNA) at different times during the ejection process at 25 °C. They are displayed in a 3D representation with time as the third axis. With a low "probability-to-reject" term in the analysis ($\sim 10^{-8}$), three separate modes are present at all times, each with its own amplitude (or area): the fast relaxation mode of the micellized receptor (mode 1) has the amplitude A_1, the intermediate phage λ mode (mode 2) amplitude A_2, and the third slower mode (mode 3) amplitude A_3. The slow mode is probably related to the low amount of DNA-capsid aggregates present in this system causing a contaminating background. These short 30 s measurements do not provide sufficiently good statistics to analyze the complete correlation functions, as reflected in the uncertainty of position of the slow mode. The amplitudes describe the relative amounts of light scattered from each component in the system, see Eq. (1), i.e., the total area of the relaxation time distribution $A_{tot}=A_1+A_2+A_3$ is equal to 1. The distributions shown in Fig. 5(a) were normalized to the count rate (or the total scattering intensity, I) and thus give the relative scattering intensity for each component ($I_1=A_1I/A_{tot}$, etc.), i.e., $I=I_1+I_2+I_3$. The relaxation time distribution at $t=0$ represents the phage λ solution at equilibrium before adding the receptor and the last distribution is obtained from a DLS measurement performed at the end of the ejection process in the mixed system. Upon carefully studying Fig. 5(a), it can be observed that after adding the receptor, the scattering resulting from the micellized receptor (fast, mode 1) and that re-

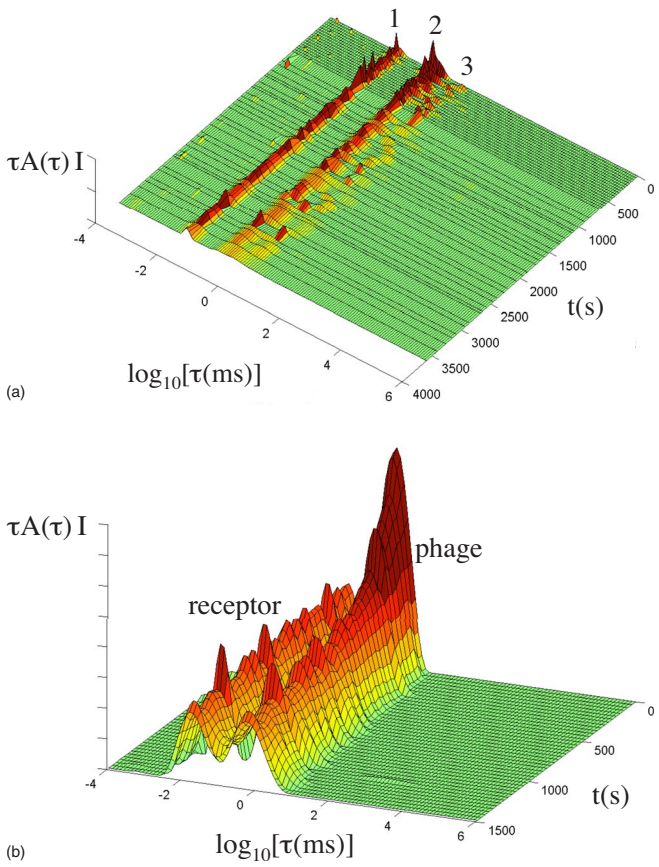

FIG. 5. (Color online) (a) The relaxation time distributions obtained from REPES with a low "probability-to-reject" term ($\sim 10^{-8}$) as a function of time during the ejection of 48.5 kbp DNA. Mode at short τ (mode 1): micellized LamB receptors, intermediate mode (mode 2): phages and mode at long τ (mode 3): DNA-capsid aggregates. (b) The relaxation time distributions obtained from REPES calculations with a "probability-to-reject" term of 0.5 as a function of time during the ejection of 48.5 kbp DNA. Mode at short τ: micellized LamB receptors and mode at long τ: phages. The distributions have been normalized by the count rate. The distributions were normalized by the count rate. (Measurements at 25 °C and at $\theta=120°$.)

sulting from the so-called aggregates (slowest, mode 3) are constant during the ejection process, and the only scattering component that changes with time is that of the phage. The scattering intensity resulting from the phage decreases with time, demonstrating a rapid decrease initially thereafter leveling off.

This can also be observed when analyzing the scattering intensities of each component, obtained from the corresponding relative amplitudes as a function of time. Although there is some uncertainty in the data for the third mode, the scattering intensity of the phage decreases, whereas the intensities of the micellized receptors and aggregates are constant. Due to the poor statistics in the third mode, which makes the REPES analysis difficult, and the fact that the scattering from the aggregates was constant, we increased the "probability-to-reject" term to 0.5. This gives bimodal relaxation time distributions with a slightly wider phage mode (mode 3 is now incorporated into the phage mode, see also Fig. 1). These distributions (normalized to the count rate) are shown in Fig. 5(b). Henceforth, the micellized receptor mode (mode 1) is denoted "receptor" (with the amplitude A_{receptor}) and the phage mode (mode 2 with mode 3 included) is denoted "phage" (with the amplitude A_{phage}). As can be seen in the figure, the mode of the receptor is constant while that of the phage changes with time.

In Fig. 4 both the DLS and SLS data for phage ejection kinetics are presented for comparison. The DLS data correspond to the light scattering intensity of the phage I_{phage} (normalized to the laser intensity and to the initial value of the total static light scattering intensity at $t=0$, I_0), I_{phage}/I_0, as a function of time. I_{phage} is obtained from the relative amplitude of the phage mode $I_{\text{phage}}=A_{\text{phage}}I/(A_{\text{receptor}}+A_{\text{phage}})$ [from the distributions in Fig. 5(b)]. In this way, the data are scaled so that the intensity varies between 0 and 1. Also shown in the figure is the normalized scattering intensity from the receptor I_{receptor}/I_0. As mentioned above, this intensity is constant over the whole duration of the measurements. Figure 4 shows the intensity change over 60 min for ejection at 25 °C. By measuring the signal again after 800 min we confirmed that the system had reached equilibrium after $\approx$80 min, since there was no change in the signal after this time.

The SLS time-resolved data are also presented in the Fig. 4 (I/I_0 vs time). It can be seen that both I/I_0 (from SLS) and I_{phage}/I_0 (from DLS) follow the same decreasing trend and are only shifted by a constant value due to the constant background scattering of the micellized receptors ($I_{\text{phage}}/I_0=I/I_0-I_{\text{receptor}}/I_0$) (see the shifted and overlapping curves in the inset of Fig. 4). This comparison shows that DLS has an advantage over SLS. With DLS it is possible to separate the contribution of each component to the total light scattering intensity during the ejection process provided that the relaxation mode corresponding to each component can be resolved from the other scattering modes (in this case the receptor and phage modes). This is not possible with the SLS technique, where the scattering intensity of the whole system is measured. This is very useful when studying the ejection kinetics in systems where more than one component that contributes to the scattering intensity change. We show it in Ref. [60], where we determine with help of DLS and SLS the rate of ejection from phage λ in the presence of DNA binding protein HU that speeds up the ejection and condenses ejected DNA into aggregates. However, for the same reason as mentioned above, and as will be discussed further, neither DLS data nor SLS can separate the scattering interference between the phage and DNA that is inside phage and outside the phage while it is being ejected, or after ejection when the DNA is in the proximity of the capsid's scattering volume. Both techniques can, however, be used in combination in order to better understand the ejection process.

C. Light scattering model of DNA ejection from the bacteriophage λ

A model is needed to describe the change in the light scattering intensity, i.e., the change in the form factor during the ejection of the DNA chain from the phage particle. Con-

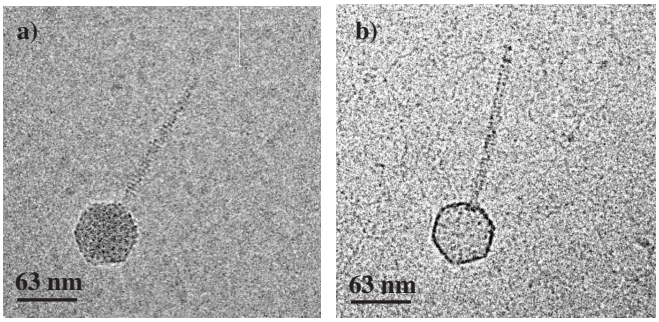

FIG. 6. Cryoelectron micrographs of (a) phage λ filled with DNA and (b) empty phage λ after 30 min incubation with LamB receptor at 37 °C. Due to the low contrast the ejected DNA is not visible with cryo EM. However, there is a clear contrast difference observed inside the phage capsid between empty and DNA filled particles.

sider a phage particle consisting of a capsid with a λ-DNA chain inside it. The capsid has a diameter of 63 nm and a thin tail 173 nm long, as seen from cryo EM micrographs in Fig. 6. Thus the total geometrical length of the phage is 236 nm. According to the SLS measurements performed in this work on three different phages containing DNA of different lengths, the R_g values were approximately 40 nm for all three cases. This indicates that the scattering from the tail does not contribute significantly since this value is close to the geometric capsid radius. As was described above, in all steps of the ejection, the scattering from oPOE micelles (with and without the LamB receptor) is constant in time, and the only contribution to the time-dependence is the scattering from the phage and the DNA that is being ejected. Therefore, in our model we will only take into account the change in scattering associated with the phage.

Consider two identical scattering elements (or centers) that are point scatterers: one located on the DNA molecule, and one on the capsid. Let us then assume that these two scattering elements may exhibit a phase relation and thus interfere. This implies a q-dependent scattering intensity, which we also observed in our SLS experiments. Due to this correlation, the total intensity $I(q)$ of the scattered light will depend on the spatial arrangement of the two scattering elements. This interference (in the case of pure intramolecular interference at infinite dilution, inside a single phage particle) is described by the form factor $P(q)$ or the particle structure factor [i.e., $I(q) \approx P(q)$] [63,64]

$$P(q) = \frac{1}{N^2} \sum_{i=1}^{N} \sum_{j=1}^{N} \langle \exp(iqr_{ij}) \rangle, \tag{6}$$

where N is the number of scattering elements (in the simple model presented here, $N=2$), r_{ij} is the magnitude of the distance vector between the scattering elements i and j: $r_{ij} = |\mathbf{r}_i - \mathbf{r}_j|$, where $\mathbf{r}_i$ and $\mathbf{r}_j$ are the coordinates of the scattering elements. The relation $\langle \exp(iqr_{ij}) \rangle = \sin(qr_{ij})/qr_{ij}$ may also be used in Eq. (6) as $\langle\ \rangle$ denotes the average of all orientations.

The ejection process is schematically illustrated in Fig. 7. For clarity, each step in the ejection of DNA is indicated in a scattering curve data versus time (shown as to scale curve taken from one of our measurements for 48.5 kbp phage at 25 °C in Fig. 4) shown in the same figure (see also Fig. 4). Step 1: Prior to receptor addition we observe the scattering from the phage capsid and the DNA that is densely packed inside it. Thus, at $t=0$, we have one scattering object (the page) consisting of two scattering elements. As mentioned above, from the determination of R_g we found that the tail does not contribute significantly to the scattering and need therefore not to be included as a scattering element in this model. The scattering intensity is then $(1+1+1+1)/2^2=1$ (multiplied by a constant) according to Eq. (6). Step 2: When the receptor is added, DNA ejection is triggered. The high internal force, originating from the close packing of the DNA, drives the ejection process. The DNA scattering element is ejected from the phage through the tail. In our model, step 2 corresponds to the situation where the capsid scattering element remains in its original position, whereas the DNA scattering element has changed its position from inside the capsid to the tip of the tail. Since the molecular weight of the scattering system has not changed after DNA is ejected, one would expect the scattering intensity not to have changed significantly directly after ejection, while the DNA is still in the direct proximity of the phage's scattering volume. However, the scattering scenario is completely different since ejection occurs through a very long tail (nearly 3 times the diameter of the capsid). This causes a change in the interference between the light scattered from the two scattering elements. Thus, in step 2, the DNA scattering element is well separated from the capsid scattering element by the long phage tail causing the two sources of scattering to become uncorrelated. Therefore, the light scattered from the DNA scattering element will not interfere with that scattered from the capsid scattering element. Using Eq. (6) and decreasing the number of scatterers to $N=1$, the scattering intensity decreases to about $(1+1)/2^2=0.5$ of the initial value. Note that we do not intend to model the scattering intensity for the situation when part of the DNA coil is inside the capsid and part is outside (an intermediate step between steps 1 and 2). This will be attempted in a future study, where the light scattering model will be developed. However, the interference between the two scatterers will change as a function of time as the DNA scattering element is transported along the tail (between steps 1 and 2). Since the uncompacted DNA chain outside the capsid scatters much less than when it is packed inside the capsid, the intensity decreases rapidly, reflecting the fact that it is in the process of leaving the capsid. Step 3: Once ejection is complete the DNA chain will slowly start to diffuse away from the phage particle. This is slow process due to the size of the DNA coil and a possible weak interaction between DNA and the capsid's exterior. Slight interference is expected between the DNA and the capsid, affecting the scattering from the capsid. During this diffusion-controlled step, the scattering intensity continues to decrease, but much more slowly than in the initial ejection step, as the form factor continues to change, slowly approaching the form factor of an empty capsid. Having adopted its normal conformation in the aqueous buffer solution away from the capsid, the ejected DNA chain will not

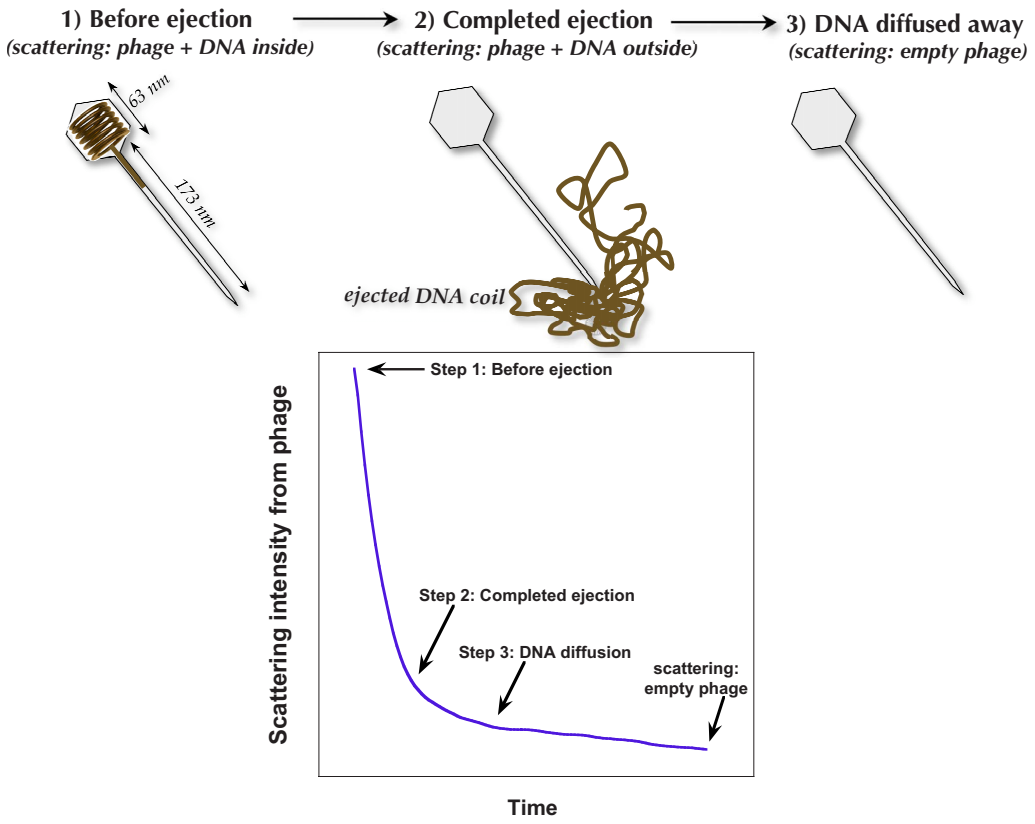

FIG. 7. (Color online) Illustration of the three major steps in the DNA ejection process from the bacteriophage λ, together with a curve showing the scattering intensity from the phage as a function of time (to scale curve taken from our measured data for 48.5 kbp phage at 25 °C).

contribute to the total scattering at an angle of 120° for two reasons: its large size and low concentration. Therefore, at the end of step 3, when only 1 scatterer remains (i.e., the capsid scattering element), the observed scattering intensity becomes constant with time, and corresponds to the scattering from an empty phage capsid. DNA filled and empty phage λ particles before and after LamB receptor addition were also imaged with cryo EM and are shown in Fig. 6.

It should be pointed out, we have assumed two scattering elements (point scatterers) and not scatterers with internal interference, which would be more appropriate when the DNA coil is ejected, and before it diffuses away from the phage particle. In addition, we have assumed a fixed relative distance instead of a pair distance distribution function (for several scattering elements), which is a coarse approximation. This model will therefore be developed in a forthcoming study. Furthermore, the time dependence of the full q-dependent scattering intensity curves during the ejection process will be analyzed.

When analyzing the scattering data obtained with DLS for ejection from the λ phage with 48.5 kbp DNA [Fig. 5(b)], the decrease in the scattering intensity of the phage with time described in the model above is indeed what we observe, see Fig. 4. It can be seen that the rapid pressure-driven DNA ejection occurs between steps 1 and 2 (during first 10 min), during which the normalized scattering intensity of the phage falls from 0.85 (at time=0) to ≈0.4, and a clear "kink" is observed in the scattering function. Thereafter, in step 3, the scattering intensity decreases slowly over 60 min, which corresponds to the slow, diffusion-controlled DNA coil translocation from the phage particle (during which the form factor approaches that of an empty capsid) and finally reaches a plateau value of ≈0.3. This slow intensity decrease in step 3 should not be attributed to the actual ejection process. However, even the ejection time between steps 1 and 2 may be a slight overestimation of the total ejection time and presents rather an upper time bond for ejection. This is because the system is better described by several point scatterers than only two. Hence, we can expect some scattering interference during the ejection process between the DNA inside and outside the capsid. Indeed, considering that the initial part of the intensity curves in Fig. 4 directly reflects the change in the fraction of unejected DNA remaining inside the capsid, implies that half of the DNA has been ejected in $t_{1/2} \approx 4$ min (where $t_{1/2}$ is the time at the half of the scattering intensity drop compared to its start value at time zero). For comparison fluorescence studies [39] showed that the ejection from λ was complete in less than a minute. However, it should also be noted that this fluorescence measurements were performed at 37 °C while our data is collected at 25 °C. Our recent DLS results have shown an exponential ejection rate dependence on the temperature with $t_{1/2} \approx 1$ min at 37 °C for wt phage λ [60]. However, both fluorescence [39] and these DLS measurements of DNA ejection kinetics show slower ejection times than the theoretically estimated value of 10 s for λ [34], thus demonstrating that the ejection rate is

strongly affected by the friction and internal interactions between DNA and capsid and tail proteins [39,60].

Also, DNA coils, empty capsids and oPOE micelles may still interact after ejection. Furthermore, it should be noted that we have earlier confirmed that DNA ejection from λ is not complete in vitro (in the absence of DNA-binding proteins), with the last, unconstrained DNA piece remaining attached to phage even after 30 min of incubation with LamB [33]. Future development of the model should allow us to establish an accurate relation between the scattering intensity and the ejected DNA fraction. However, the initially recorded change in the scattering intensity does reflect the change in the fraction of unejected DNA, and we can therefore use these kinetic data to estimate the initial ejection rate. Specifically, we used the DLS and SLS methods in our recently published work [60], to internally compare the initial rate of DNA ejection from bacteriophage λ under various internal and external conditions, varying such parameters as temperature, packaged DNA length and also adding DNA-binding proteins to the host solution (HU and DNase I) [60].

IV. CONCLUSIONS

Dynamic light scattering has been used to study the ejection of DNA from bacteriophage λ. We found this technique to have a major advantage over the fluorescence and SLS techniques, since it allows the study of the change in the absolute scattering intensity of each component in the system as a function of time. The individual scattering intensities were obtained by using the pre-exponential amplitudes obtained from the inverse Laplace transformation of the time correlation function of the scattered intensity obtained from a time-resolved DLS experiment. From the DLS measurements performed in this study, we were able to conclude that it is the change in the light scattering from the phage that is responsible for the overall change in the total light scattering intensity during the ejection process, while the light scattered by the other components remained constant.

Using SLS measurements we obtained the same form factor (or almost the same) for phages with different DNA chain lengths, which indicates that the form factor of the phage capsid is determined by the capsid geometry, and that the scattering signal depends mainly on the length of the confined DNA chain. However, when the ejection process is initiated by receptor addition, the observed decrease in light scattering intensity is related to the change in the form factor of the phage particle through the intraparticle interference between the phage capsid and the DNA.

In this work we also present a model explaining why light scattering measurements of phage DNA ejection are possible on bacteriophages. This model shows that because of the long tail of the phage there is very little scattering interference between the ejected DNA and the capsid, and we therefore observe a rapid decrease in the scattering signal during the ejection process. If the phage tail were much shorter, as in the case of bacteriophage $\phi 29$, no significant change in the scattering intensity would probably be observed during DNA ejection. However, immediately after ejection, while the ejected DNA is close to the phage, it will still contribute slightly to the capsid's scattering intensity through weak scattering interference. Due to the size of the DNA chain and low concentration, the ejected DNA coil will no longer contribute to the total scattering intensity once it has diffused away from the scattering volume of the phage capsid. The signal then originates from the scattering of an empty capsid plus a constant background arising from scattering from surfactant micelles, with and without the receptor.

In both DLS and SLS measurements, we have shown that the changes in the scattering intensity are directly associated with the DNA ejection from the phage. Hence, this method can be used in the future to compare the initial ejection rates under various internal and external conditions within the same phage system. The analysis method based on the dynamic light scattering technique developed in this work will allow us to study the forces controlling the rate of ejection as we try to influence them by, for instance, changing the temperature, varying the length of the packed genome or through the addition of DNA-binding proteins to the host solution, which we demonstrate in [60].

ACKNOWLEDGMENTS

Petr Štěpánek is kindly acknowledged for providing the REPES program and for fruitful discussions. The authors are grateful to Meerim Jeembaeva for help with sample preparation and to Daniel Angelesco for his input in various ways. We acknowledge the financial support of the Swedish Research Council (A.E.) and the Swedish Linneus Center of Excellence, "Organizing Molecular Matter" (K.S.).

[1] V. A. Bloomfield, Annu. Rev. Biophys. Bioeng. **10**, 421 (1981).
[2] V. A. Bloomfield, in *Dynamic Light Scattering: Applications of Photon Correlation Spectroscopy*; edited by R. Pecora (Plenum Press, New York, 1985), p. 363.
[3] *Laser Light Scattering in Biochemistry*; edited by S. E. Harding, D. B. Sattelle, and V. A. Bloomfield (The Royal Society of Chemistry, Cambridge, 1992).
[4] P. A. Janmey, in *Dynamic Light Scattering: The Method and Some Applications*, edited by W. Brown (Oxford University Press, Oxford, 1993), p. 611.
[5] T. Liu and B. Chu, in *Encyclopedia of Surface and Colloid Science*, edited by A. Hubbard (Marcel Dekker, New York, 2002); p. 3023.
[6] S. S. Sorlie and R. Pecora, Macromolecules **21**, 1437 (1988).
[7] S. S. Sorlie and R. Pecora, Macromolecules **23**, 487 (1990).
[8] J. Seilst and R. Pecora, Macromolecules **28**, 661 (1995).
[9] M. A. Ivanova, A. V. Arutyunyan, A. V. Lomakin, and V. A. Noskin, Appl. Opt. **36**, 7657 (1997).
[10] H. Liu, J. Gapinski, L. Skibinska, A. Patowksi, and R. Pecora,

J. Chem. Phys. **113**, 6001 (2000).
[11] S. He, P. G. Arscott, and V. A. Bloomfield, Biopolymers **53**, 329 (2000).
[12] R. S. Dias, A. A. C. C. Paisa, M. G. Miguel, and B. Lindman, Colloids Surf., A **250**, 115 (2004).
[13] D. McLoughlin, M. Delsanti, C. Tribet, and D. Langevin, Europhys. Lett. **63**, 461 (2005).
[14] M. Cárdenas, K. Schillén, T. Nylander, J. Jansson, and B. Lindman, Phys. Chem. Chem. Phys. **6**, 1603 (2004).
[15] M. Cárdenas, K. Schillén, D. Pebalk, T. Nylander, and B. Lindman, Biomacromolecules **6**, 832 (2005).
[16] R. S. Dias, J. Innerlohinger, O. Glatter, M. G. Miguel, and B. Lindman, J. Phys. Chem. B **109**, 10458 (2005).
[17] M. Cárdenas, J. Barauskas, K. Schillén, J. L. Brennan, M. Brust, and T. Nylander, Langmuir **22**, 3294 (2006).
[18] M.-L. Öberg, K. Schillén, and T. Nylander, Biomacromolecules **8**, 1557 (2007).
[19] R. W. Hendrix, J. W. Roberts, F. W. Stahl, and R. A. Weisberg, *Lambda II* (Cold Spring Harbor Lab Press, Woodbury, NY, 1983).
[20] D. G. Angelescu, R. Bruinsma, and P. Linse, Phys. Rev. E **73**, 041921 (2006).
[21] A. J. Spakowitz and Z.-G. Wang, Biophys. J. **88**, 3912 (2005).
[22] C. Forrey and M. Muthukumar, Biophys. J. **91**, 25 (2006).
[23] I. Ali, D. Marenduzzo, and J. M. Yeomans, Phys. Rev. Lett. **96**, 208102 (2006).
[24] S. C. Reimer and V. A. Bloomfield, Biopolymers **17**, 785 (1978).
[25] J. T. Kindt, S. Tzlil, A. Ben-Shaul, and W. M. Gelbart, Proc. Natl. Acad. Sci. U.S.A. **98**, 13671 (2001).
[26] S. Tzlil, J. T. Kindt, W. M. Gelbart, and A. Ben-Shaul, Biophys. J. **84**, 1616 (2003).
[27] P. K. Purohit, J. Kondev, and R. Phillips, Proc. Natl. Acad. Sci. U.S.A. **100**, 3173 (2003).
[28] P. K. Purohit, J. Kodnev, and R. Phillips, J. Mech. Phys. Solids **51**, 2239 (2003).
[29] P. K. Purohit, M. M. Inamdar, P. D. Grayson, T. M. Squires, J. Kondev, and R. Philips, Biophys. J. **88**, 851 (2005).
[30] A. Evilevitch, L. Lavelle, C. M. Knobler, E. Raspaud, and W. M. Gelbart, Proc. Natl. Acad. Sci. U.S.A. **100**, 9292 (2003).
[31] A. Evilevitch, M. Castelnovo, C. M. Knobler, and W. M. Gelbart, J. Phys. Chem. B **108**, 6838 (2004).
[32] D. E. Smith, S. J. Tans, S. B. Smith, S. Grimes, D. L. Anderson, and C. Bustamante, Nature (London) **413**, 748 (2001).
[33] A. Evilevitch, J. Phys. Chem. B **110**, 22261 (2006).
[34] M. M. Inamdar, W. M. Gelbart, and R. Phillips, Biophys. J. **91**, 411 (2006).
[35] In *Escherichia coli and Salmonella typhimurium*, edited by F. Neidhardt (ASM Press, Washington, D.C., 1996).
[36] P. Grayson, A. Evilevitch, M. M. Inamdar, P. K. Purohit, W. M. Gelbart, C. M. Knobler, and R. Phillips, Virology **348**, 430 (2006).
[37] M. de Frutos, L. Letellier, and E. Raspaud, Biophys. J. **88**, 1364 (2005).
[38] M. de Frutos, S. Brasiles, P. Tavares, and E. Raspaud, Eur. Phys. J.: Appl. Phys. **E17**, 429 (2005).
[39] S. L. Novick and J. D. Baldeschwieler, Biochemistry **27**, 7919 (1988); S. Mangenot, M. Hochrein, J. Radler, and L. Letellier, Curr. Biol. **15**, 430 (2005).
[40] M. Eriksson, M. Härdin, A. Larsson, J. Bergenholtz, and B. Åkerman, J. Phys. Chem. B **111**, 1139 (2007).
[41] T. J. Silhavy, in *Experiments with Gene Fusions*, edited by T. J. Silhavy, M. L. Berman, and L. W. Enquist (Cold Spring Harbor Laboratory, Cold Spring Harbor, NY, 1984).
[42] A. Graff, M. Sauer, P. van Gelder, and W. Meier, Proc. Natl. Acad. Sci. U.S.A. **99**, 5064 (2002).
[43] M. Roa and D. Scandella, Virology **72**, 182 (1976).
[44] L. Randall-Hazelbauer and M. Schwartz, J. Bacteriol. **116**, 1436 (1973).
[45] M. Roa, FEMS Microbiol. Lett. **11**, 257 (1981).
[46] A. Prilipov, P. S. Phale, P. Van Gelder, J. P. Rosenbusch, and R. Koebnik, FEMS Microbiol. Lett. **163**, 65 (1998).
[47] J. Jansson, K. Schillén, G. Olofsson, R. C. da Silva, and W. Loh, J. Phys. Chem. B **108**, 82 (2004).
[48] A. J. F. Siegert, MIT Rad. Lab. Rep. No. 465 (1943).
[49] P. Stepanek, in *Dynamic Light Scattering: The Method and Some Applications*; edited by W. Brown (Oxford University Press, Oxford, 1993), p. 177.
[50] J. Jakeš, Czech. J. Phys., Sect. B **38**, 1305 (1988).
[51] J. Jakeš, Collect. Czech. Chem. Commun. **60**, 1781 (1995).
[52] K. Schillén, W. Brown, and R. M. Johnsen, Macromolecules **27**, 4825 (1994).
[53] P. Štěpánek (private communication).
[54] T. Dokland and H. Murialdo, J. Mol. Biol. **233**, 682 (1993).
[55] *Light Scattering: Principles and Development*, edited by W. Brown (Clarendon Press, Oxford, 1996).
[56] K. Schillén, J. Jansson, D. Löf, and T. Costa (to be published).
[57] W. Burchard, Macromol. Chem. Phys. **39**, 179 (1990).
[58] W. Burchard and W. Richtering, Prog. Colloid Polym. Sci. **80**, 151 (1989).
[59] W. Burchard, in *Light Scattering: Principles and Development*, edited by W. Brown (Clarendon Press, Oxford, 1996), p. 439.
[60] D. Löf, K. Schillén, B. Jönsson, and A. Evilevitch, J. Mol. Biol. **368**, 1 (2007).
[61] This fact, in addition to the low concentration, explains why no relaxation process of the free DNA is observed in the DLS measurements on the phage system. Attempts were also made to measure DLS on pure λ-DNA in bulk solution with the same concentration as the ejected DNA in our phage system but the scattering intensity was too low, confirming our assumption above. Even an attempt to increase DNA concentration by 100 times and decrease to $\theta=35°$ was unsuccessful.
[62] S. N. Slilaty, K. I. Berns, and H. V. Aposhian, J. Biol. Chem. **257**, 6571 (1982).
[63] K. S. Schmitz, *An Introduction to Dynamic Light Scattering by Macromolecules* (Academic Press, San Diego, 1990).
[64] *Neutron, X-ray and Light: Scattering Methods Applied to Soft Matter*, edited by P. Lindner and T. Zemb (Elsevier Science, Amsterdam, 2002).